Showa Univ J Med Sci **32**(3), 193～206, September 2020

Original

C-arm Cone-beam CT-guided Needle Biopsies through the Erector Spinal Muscle for Posterior Thoracic Pulmonary Lesions

Nobuyuki TAKEYAMA*[1)], Toshi HASHIMOTO[1)], Akio KOTAKE[1)], Yoshiro HORI[1)], Yuki TASHIRO[1)], Takaki HAYASHI[2)], Kota WATANABE[2)], Tomohide ISOBE[3)], Tomoko NOROSE[3)] and Nobuyuki OHIKE[3)]

Abstract: This study investigated retrospectively the diagnostic yield and complication rate of transthoracic needle biopsies for posterior thoracic pulmonary lesions using C-arm cone-beam computed tomography (CBCT). The risk factors for pulmonary hemorrhage were evaluated. Our study included 113 patients with 113 posterior pulmonary lesions (mean longest diameter: 30.6 mm, and mean depth: 4.7 mm) through the erector spinal muscles using a 19 / 20-gauge coaxial system. The diagnostic performances of procedures for malignant lesions and the incidence of complications after biopsies were also assessed. The patient-related and procedure-related variables were investigated. Risk factors for pulmonary hemorrhage were analyzed with a multivariate logistic regression analysis. Findings revealed 99 malignant, 13 benign, and one intermediate lesion. Sensitivity, specificity, and diagnostic accuracy rates were 100% (99 / 99), 92.3% (12 / 13), and 99.1% (111 / 112), respectively. Air embolization, hemothorax, hemoptysis, pneumothorax, and pulmonary hemorrhage, occurred in 0, 2, 12, 48, and 70 procedures. The averaged spinous process-pleura depth and the traversed lung parenchyma depth achieved by the introducer needles were 54.2 mm and 27.4 mm, respectively. The needle position at the pleural puncture site within the intercostal space was in middle (31%) and inferior (69%) areas. The incidence of pulmonary hemorrhage was significantly higher in smaller lesions ($p=0.001$). Manual evacuation was performed in five procedures for patients with pneumothorax. The chest tube placement (trocar > 8 Fr) was performed in two procedures in patients with hemothorax and pneumothorax. In conclusion, the biopsy method with a posterior intercostal approach for posterior thoracic pulmonary lesions yielded high diagnostic accuracy and few major complications.

Key words: CBCT, biopsy, pulmonary hemorrhage, intercostal space

Introduction

Computed tomography (CT)-guided percutaneous transthoracic lung biopsy (TLB) is a well-established, minimally invasive technique used to characterize pulmonary lesions that are

[1)] *Department of Radiology, Showa University Fujigaoka Hospital,* 1-30 Fujigaoka, Aoba-ku, Yokohama 227-8501, Japan.
[2)] *Department of Radiology, Showa University Northern Yokohama Hospital.*
[3)] *Department of Pathology and Laboratory Medicine, Showa University Fujigaoka Hospital.*
* To whom corresponding should be addressed.

suspicious of malignancy and inaccessible by bronchoscopy[1]. This procedure is conventionally performed with CT fluoroscopy and CT-guidance, and it has achieved a high-diagnostic accuracy (> 90%) and increased sensitivity and specificity (both > 95%) in diagnosing malignancies[2].

C-arm cone-beam CT (CBCT) was introduced recently because the CBCT system enables both fluoroscopic and CT-guidance using a cone-beam X-ray tube and a flat-panel detector[3], wherein CBCT-guided TLB procedures can yield similar diagnostic accuracy and complications to CT-fluoroscopic biopsies[4, 5].

Several approaches can be used in TLB for the posterior thoracic pulmonary lesions, namely, posterior, posterolateral, and lateral approaches. The most posterior approach is performed through the intercostal space via the erector spinal muscles. Needle progression through the posterior thoracic wall can achieve good needle stabilization[6]. However, there is a potential risk of hemothorax secondary to laceration of the posterior intercostal artery (PIA) during needle insertion into the intercostal space[7–10].

Recently, several researchers have investigated the anatomical course of the PIA along the 4th to the 11th intercostal spaces on CT angiography[9, 10]. The authors of these studies recommended that the needle should not be progressed in the posterior paravertebral space and within the first 6 cm lateral to the spine because the PIA moves away from the costovertebral junction and has a meandering path in the inferior half of the intercostal space in the medial chest[8–10]. The ideal posterior intercostal approach should be performed by allowing needle traversal along the superior cortex of the lower rib to avoid hemothorax[11–13]. However, there are no published data with CBCT-based, three-dimensional (3D) needle guidance. Based on previous reports, we attempted to position the pleural puncture point at approximately 6 cm lateral to the spinous process at all spinal levels.

The purpose of this study was a) to investigate the diagnostic yield for malignancy and the complication rate in our CBCT-guided TLB procedure with a posterior intercostal approach through the erector spinal muscles, and b) to assess the pleural puncture point quantitatively and qualitatively. In addition, the variables that influence pulmonary hemorrhage were evaluated using univariate and multivariate logistic regression analyses.

Methods

Patients

The Institutional Review Board of the Fujigaoka Hospital at the Showa University approved this retrospective study (permission number F2019C72), and waived the requirement for informed consent. From August 2013 to August 2019, 201 consecutive CBCT-guided TLBs were performed for intrathoracic lesions in 201 patients to acquire the tissues before therapeutic planning.

The indication criteria for TLB were peripherally located pulmonary lesions in patients who underwent recent diagnostic CT (no more than 2 months) and nondiagnostic bronchoscopy prior to TLB[4]. In addition, inclusion criteria for biopsy included lesions with maximum diameters > 8 mm[14, 15], and patients who suffered from refractory coagulopathy (internally normalized ratios < 1.5 or thrombocyte counts > 100,000 /mm^3). Lesions which were suspected to have vascular origin, and severe respi-

ratory disease, namely, advanced emphysema and advanced interstitial pulmonary disease, were excluded. Anticoagulants or antithrombotics, such as aspirin and clopidogrel, were withheld for 7 days, and heparin was withheld for 1 day before TLB.

From the total number of TLBs (n=201), 81 procedures conducted with an anterior approach and seven with a posterolateral approach through the intercostal space were excluded. By contrast, 113 TLBs performed on intrathoracic lesions with a posterior approach through the erector spinal muscles were included in this study.

The patient baseline data and the characteristics of their pulmonary lesions are summarized in Table 1. The lesion size was measured along the longest diameter, and the lesion depth was measured as the shortest distance between the lesion and the pleural surface (not the depth along the planned needle path) using axial CT images[13].

Table 1. Characteristics of 113 pulmonary lesions in 113 patients

Characteristics	Value (range)
Age (year)	69.4±9.3 (40-84)
Sex: male / female	80 / 33
Lesion location	
(right lobe) Upper / Middle / Lower	(right lobe) 31 / 16 / 23
(left lobe) Upper / Middle / Lower	(left lobe) 12 / 14 / 17
Peripheral / Nonperipheral	105 / 8
Paramediastinal / Nonparamediastinal	36 / 77
Lesion consistency	
Ground-glass opacity / Partly solid / Solid	4 / 4 / 105
Cavitation or dilated bronchi within the lesion (yes / no)	13 / 100
Lesion size	
The longest diameter	30.6±19.8 (8.8-117)
<10 / 10-20 / 20-30 / 30-40 / >40 mm	4 / 38 / 33 / 13 / 25
Lesion depth (mm)	4.7±8.6 (0-48)
Relation with the pleura: abutting / ≤ 20 / >20	67 / 38 / 8
Number of procedures at each intercostal space	
2^{nd} / 3^{rd} / 4^{th} / 5^{th} / 6^{th} / 7^{th} / 8^{th} / 9^{th} / 10^{th} / 11^{th}	7 / 17 / 14 / 8 / 7 / 14 / 10 / 23 / 10 / 1
Patient position at biopsy	
Right posterior oblique / left posterior oblique / horizontal	50 / 25 / 38
Needle position at the pleural puncture site within the intercostal space:	
Superior / Middle / Inferior	0 / 35 / 78
Direction of the needle progression	
Craniocaudal / caudocranial / axial	49 / 42 / 22
Mediolateral / lateromedial / perpendicular	71 / 29 / 13
Distance from the spinous process to the pleura (mm)	
Entire thoracic spine (2^{nd} to 11^{th} intercostal spaces)	54.2±14.5 (20-95)
2^{nd} to 3^{rd} intercostal spaces (n=24)	50.3±11.6 (38-75)
4^{th} to 7^{th} intercostal spaces (n=45)	52.2±14.8 (20-90)
8^{th} to 11^{th} intercostal spaces (n=44)	58.2±14.7 (40-95)
Distance of traversed lung parenchyma (mm)	27.4±15.0 (3-70)
≤ 15 mm / >15 mm left inside the lung parenchyma	31 / 82
Presence of emphysema (yes / no)	49 / 64

Qualitative data: number; Quantitative data: mean±standard deviation (SD) (range)

Biopsy Procedure

Two interventional radiologists (R1 and R2 who have respective image-guided biopsy experiences of 35 years and 22 years) and five general radiologists (R3, R4, R5, R6, and R7, who have respective image-guided biopsy experiences of 32 years, 20 years, 10 years, 5 years, and 4 years) performed TLB procedures with a CBCT system (Allura Clarity FD2020, Philips Medical System, Best, The Netherlands). A coaxial system was used with an introducer (19-gauge) and an automated cutting needle (20-gauge, Quick Core Biopsy Set, Cook, Bloomington, IN, USA) with a penetration depth of 20 mm. Each patient was positioned in prone position in the right posterior oblique (n=50), left posterior oblique (n=25), or horizontal (n=38) directions according to the access route.

The first step involved the acquisition of 3D data and the planning of the needle trajectory using software at a computer workstation (XperGuide and XperVision, Philips Healthcare). Thin slices (slice thickness of 0.66 mm) were acquired with CBCT scans with a 512×396 matrix size and 210 rotations in 5.2 s around the region of interest at the end of expiration. Once the target point and skin entry point were established, a safe trajectory route was determined with a centimeter scale on axial and oblique sagittal views. Lesions were approached in such a way to avoid a) interlobular fissures or the superior intercostal space, and b) striking visible bronchi, vessels, or severe emphysema and cavitation.

The second step involved the advancement of the coaxial system with virtual fluoroscopic guidance. The access area was cleaned first, and local anesthesia was applied. Following the virtual path with fluoroscopy from the skin entry site to the target lesion as a bull's-eye map (Fig. 1), the needle tip was placed at the cutaneous entry point and was advanced at a depth of 3–4 cm into the subcutaneous tissue and erector spinal muscles just proximal to the parietal pleura. In some patients, we used wet gauze swabs to support the needle. After the coaxial tip reached the proper position at the pleural puncture point on CBCT, the parietal pleura was traversed with a single puncture, and an introducer was placed in front of, or within the lesion.

Finally, a cutting needle was exchanged from the introducer and a core biopsy was conducted at the end of expiration after the accurate localization of the introducer tip was confirmed using axial, oblique sagittal, and coronal images on CBCT. When the specimen was macroscopically assessed, multiple samples (2–4 additional biopsies) were performed from a different part of the lesion by tilting the extrathoracic portion of the introducer at every needle pass[16, 17].

If cavitation and dilated bronchi were within the lesion, the introducer was advanced to the solid component of the lesion (Fig. 2).

After the coaxial system was removed, the CBCT images were obtained after the procedure with the same parameters as those used before the procedure to assess any biopsy-related complications, namely, air embolization, hemothorax, pneumothorax, pulmonary hemorrhage, and hemoptysis. Patients remained under observation in the hospital until the subsequent morning.

An erect chest radiograph was performed 4 h after the procedure to detect any complications. In patients with marked changes in vital signs or clinical status, repeated imaging was indicated.

The criteria for the manual evacuation through the intercostal space during the procedure with an 18-gauge catheter included symptomatic or stable pneumothorax with lung retraction distances $>$ 2 cm.

The criteria associated with chest tube placements included symptomatic pneumothorax at the post-CBCT procedure. When the hemothorax appeared during the procedure, TLB continued to acquire the tissue if the pleural blood effusion did not increase or the patient did not show symptoms, such as dyspnea and thoracic pain. When the post-CBCT procedure demonstrated increasing volume of blood effusion, an intercostal chest tube was inserted.

Data collection and statistical analyses

We collected radiological reports, histological data, and medical records for each procedure. Technical success was defined as the successful positioning of the cutting needle tip within the lesion before biopsy and the adequate sampling of the biopsy specimen.

The pathological reports of biopsy specimens, surgical specimens, or follow-up images were reviewed to evaluate the final diagnosis of the target nodules[13]. The final diagnosis (Table 2)

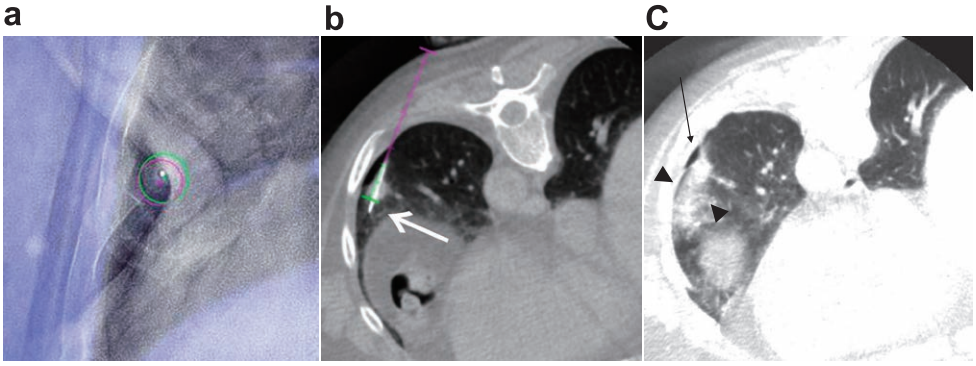

Fig. 1. A 12 mm nodule in the left lower lobe in a 62-year-old woman
a : Virtual-guided planning for a safe needle route to a target lesion (green circle) and the entry site (purple circle) that are aligned vertically.
b : After advancing the introducer along the safe trajectory route (red line) the position of the needle tip is confirmed to lie within the target lesion (arrow) on axial, C-arm, cone beam, computed tomography (CBCT) images.
c : Axial CBCT image acquired after the procedure showing hemorrhage (>2 cm) as a perilesional consolidation (arrowheads) with a small amount of pneumothorax (arrow). The lesion was confirmed to be squamous cell carcinoma.

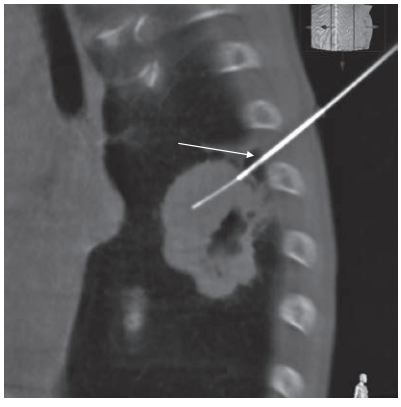

Fig. 2. A 38 mm tumor in the right lower lobe in a 71-year-old man
The oblique CBCT image shows that the cutting needle has been advanced to the solid component of the lesion to avoid hitting the cavity. The needle is advanced at the inferior area (arrow) at the pleural puncture site within the 5th intercostal space in a head-tail direction. The lesion was confirmed to be small cell carcinoma.

Table 2. Pathological confirmation

Classification	Pathological confirmation	Number
Malignant (n=99)	Adenocarcinoma	48
	Squamous cell carcinoma	26
	Small cell carcinoma	11
	Metastatic tumor	7
	Large cell carcinoma	3
	Diffuse large B cell lymphoma	2
	[a]MALT lymphoma	1
	Sarcomatoid tumor	1
Benign (n=13)	Epithelioid granuloma	4
	Organizing pneumonia	3
	Inflammatory cell infiltration with fibrosis	1
	Tuberculosis	1
	Hamartoma	1
	Plasmacytoma	1
	Amyloidosis	1
	Atypical cell infiltration	1
Indeterminate	Inflammatory cell infiltration	1

[a]MALT: mucosa-associated lymphoid tissue

was confirmed according to following: (a) if patients underwent surgical resection, pathological reports determined the final diagnosis. (b) If the pathological biopsy results demonstrated a malignant or a specific benign pathology, such as tuberculosis, hamartoma, plasmacytoma, and amyloidosis, the outcome was accepted as the final diagnosis. (c) In the cases of nonspecific benign pathology, including chronic inflammation or fibrosis, follow-up CT helped decide whether the lesion would be truly or falsely benign, or indeterminate. If lesions decreased in diameter by 20% or more during follow-up periods or appeared unchanged for >2 years, we considered the final diagnosis as benign[10]. (d) If a nodule with nonspecific benign pathology did not show sufficient decrease in size, or was not able to be tracked by follow-up images, its final diagnosis was defined as indeterminate. Indeterminate lesions were excluded from the evaluation of the diagnostic yield. Sensitivity, specificity, and accuracy for malignant lesions were then analyzed.

Intercostal spaces were divided into three parts (upper, middle, and inferior) as follows[6]: Upper, 2nd to 3rd intercostal spaces in which PIAs were small and invisible above the lower margin of the scapula; Middle, 4th to 7th, and Inferior, 8th to 11th intercostal spaces in which PIAs were visible below the scapula.

Complications, including air embolization, hemothorax, hemoptysis, pneumothorax, and pulmonary hemorrhage were assessed after TLB[18–25]. Pulmonary hemorrhage was defined as a new consolidation or ground-glass opacity in after the CBCT procedure, including perilesional hemorrhage and needle tract hemorrhage[8]. The severity of pulmonary hemorrhage was categorized as grade 1 if the hemorrhage had a width ≤ 2 cm for needle tract hemorrhage and perilesional hemorrhage, grade 2 when lesions had widths >2 cm, and grade 3 when lobar or greater hemorrhage occurred[26]. Hemoptysis was graded as either mild when it was limited to the hemoptoic

sputum, or as abundant[27]. The degree of pneumothorax was graded during the procedure as mild pneumothorax when it resulted in a lung surface retraction of 2 cm, moderate pneumothorax when it caused lung retraction for a distance between 2 and 4 cm, and severe pneumothorax when it caused retraction of the pulmonary surface by more than 4 cm[19].

Patient demographics and technical parameters that could influence the frequency of pulmonary hemorrhage (Table 3) and pneumothorax (Table 4) were also investigated.

Statistical analyses

Statistical data analyses were performed with SPSS (version 26, IBM, Armonk, NY, USA). The chi-square test was used for categorical variables, and the Student's t-test was used to analyze continuous variables to compare patients with and without pulmonary hemorrhage. Candidate variables with $p < 0.10$ in the univariate analyses were included in the multivariate logistic regression. Only the factors which were statistically significant based on multivariate analyses were considered independent risk factors. A p-value < 0.05 was considered statistically significant. All data are shown as mean values ± standard deviations.

Table 3. Relationships of pulmonary hemorrhage and patient technical parameters

Quantitative and qualitative parameters	Without pulmonary hemorrhage (n=43)	With pulmonary hemorrhage (n=70)	Univariate p value	Multivariate B	Multivariate Exp (B)	Multivariate p value
Age (year)	70.8±8.4	68.3±9.7	0.175			
Sex (male / female)	32 / 11	47 / 23	0.413			
Presence of emphysema (yes / no)	21 / 22	27 / 43	0.190			
Lesion location						
Right / Left	27 / 16	43 / 27				
Upper / Middle / Lower lobes	16 / 11 / 16	27 / 19 / 24	0.885 0.950			
Peripheral / Nonperipheral	40 / 3	64 / 6	0.761 0.589			
Paramediastinal / Nonparamediastinal	15 / 28	21 / 49				
Morphologic characteristics						
GGO[a] / partly solid / solid / consolidation	1 / 0 / 33 / 9	3 / 5 / 55 / 7	0.132 0.237			
Cavity (yes / no)	3 / 40	10 / 60				
Lesion size	46.2±22.4	20.8±8.9	**< 0.001**	**−0.118**	**0.889**	**< 0.001**
Lesion depth (mm)	2.5±8.6	6.0±8.3	**0.038**	0.014	1.014	0.655
Spinous-process-pleural-depth (mm)	53.6±17.4	54.3±12.5	0.812			
Traversed lung parenchyma depth (mm)	23.1±14.5	30.0±14.7	**0.017**	0.014	1.014	0.451
Skin-surface-pleural-depth (mm)	38.5±13.2	41.2±12.0	0.277			
Patient position at biopsy						
Right posterior oblique / left posterior oblique / horizontal	19 / 6 / 18	31 / 19 / 20	0.174			
Direction of the needle progression						
Craniocaudal / caudocranial / axial	21 / 14 / 8	27 / 28 / 15	0.559 0.445			
Mediolateral / lateromedial / perpendicular	11 / 25 / 7	18 / 46 / 6				
Needle position at the pleural puncture site within the intercostal space (middle / inferior)	12 / 31	23 / 47	0.581			

[a]GGO: ground-glass opacity

Table 4. Relationship of pneumothorax and patient technical parameters

Quantitative and qualitative parameters	Without pneumothorax (n=63)	With pneumothorax (n=50)	Univariate p value	Multivariate B	Multivariate Exp (B)	Multivariate p value
Age (year)	67.8±10.0	71.2±8.0	**0.048**	0.067	1.069	**0.013**
Sex (male / female)	46 / 17	33 / 17	0.419			
Presence of emphysema (yes / no)	22 / 41	27 / 23	**0.042**	0.805	2.237	0.089
Lesion location						
Right / Left	42 / 21	28 / 22				
Upper / Middle / Lower lobes	28 / 14 / 21	15 / 16 / 19	0.246 0.259			
Peripheral / Nonperipheral	57 / 6	47 / 3	0.492 0.110			
Paramediastinal / Nonparamediastinal	24 / 39	12 / 38				
Morphologic characteristics						
GGO[a] / partly solid / solid / consolidation	2 / 2 / 52 / 7	2 / 3 / 36 / 9	0.596 0.182			
Cavity (yes / no)	5 / 58	8 / 42				
Lesion size	34.8±22.7	25.2±13.8	**0.011**	−0.040	0.961	**0.008**
Lesion depth (mm)	4.4±7.9	5.1±9.4	0.650			
Spinous-process-pleural-depth (mm)	52.4±15.0	56.1±13.6	0.188			
Traversed lung parenchyma depth (mm)	26.4±14.2	28.5±16.2	0.463			
Skin-surface-pleural-depth (mm)	39.6±12.2	40.9±13.0	0.574			
Patient position at biopsy						
Right posterior oblique / left posterior oblique / horizontal	22 / 15 / 26	28 / 10 / 12	**0.065**	−1.102	0.322	0.064
Direction of the needle progression						
Craniocaudal / caudocranial / axial	21 / 31 / 11	21 / 17 / 12	0.264			
Medial-lateral / lateral-medial / perpendicular	22 / 30 / 11	7 / 41 / 2	**0.001**	1.702	5.484	**0.002**
Needle position at the pleural puncture site within the intercostal space (middle / inferior)	18 / 45	17 / 33	0.535			

[a]GGO: ground-glass opacity

Results

In the quantitative assessments (Table 1), the lesion size was 30.6 ± 19.8 mm (range from 8.8–117 mm). In addition, 43, 30, and 40 lesions were located in the upper, middle, and lower lobes, and ground-glass opacity (n=4), partly solid (n=4), and solid (n=105) lesions were detected. The lesion depth was 4.7 ± 8.6 mm (range from 0–48 mm). The numbers of lesions that abutted the pleura, ≤20 mm from the pleura, and >20 mm from the pleura, were 67, 38, and 8, respectively; 105 / 113 (92.9%) lesions were positioned peripherally, and eight were nonperipheral. Thirty six of 113 (31.9%) lesions were located in the paramediastinum, and 77 were nonparamediastinal. The number of procedures performed to advance the introducers via the 2nd, 3rd, 4th, 5th, 6th, 7th, 8th, 9th, 10th, and 11th intercostal spaces were 7, 17, 14, 8, 7, 14, 10, 23, 10, and 1, respectively. In addition, the mean distances from the spinous processes to the pleura (Fig. 3) were 54.2 ± 14.5 mm for all intercostal spaces, 50.3 ± 11.5 mm via the 2nd to the 3rd intercostal spaces, 52.1 ± 14.8 mm via the 4th to the 7th, and 58.1 ± 14.7 mm via the 8th to the 11th intercostal spaces. Regarding the set goal for the distance from the spinous processes of > 6 cm, 35 of 113 (30.9%) procedures fulfilled the requirement: 5 of 24 (20.8%) were in the 2nd the 3rd intercostal spaces, 11 of 45 (24.4%) were in the 4th to 7th intercostal spaces, and 19 of 44 (43.2%) were in

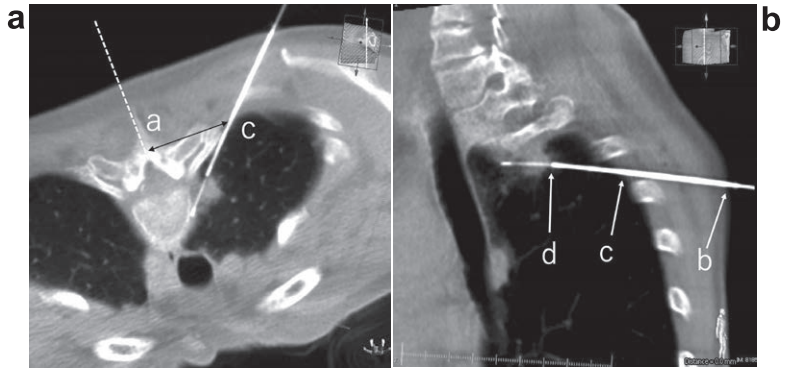

Fig. 3. 13 mm nodule in the apex of the right lobe in a 59-year-old woman. The lesion was confirmed to be adenocarcinoma

a : Axial CBCT image showing that the cutting needle penetrated into the target lesion in the lateral to medial direction. The distance from the spinous process to the pleura was measured from the dotted line parallel to the spinous process to the pleura, at the puncture site (distance from a to c).

b : The oblique sagittal image shows that the distance from the pleura at the puncture site (distance from c to d), and the distance from the skin surface at the pleura was measured from the skin surface at the entry site to the pleura at the puncture site (distance from b to c).

the 8th to the 11th intercostal spaces. The mean distance of traversed lung parenchyma was 27.4 ± 15.0 mm, and the mean distance of the skin surface to the pleura was 40.2 ± 12.5 mm.

Regarding the qualitative evaluation, the pleural puncture points in the intercostal space were classified as the middle (n=35) and inferior (n=78) areas. No procedures involved the advancement of the needle in the superior area within the intercostal space. Regarding the direction of needle progression, the numbers of procedures performed along the head-tail, tail-head, and horizontal progression directions were 49, 42, and 22, respectively. In addition, the numbers of medial-lateral, lateral-medial, and vertical progressions were 71, 29 and 13, respectively.

The technical success rate, defined as the provision of an adequate sample for diagnosis, was 113 / 113 (100%) in this study. Histological results for the TLB procedures are summarized in Table 2. Ninety-nine (87.6%) biopsies (from the total of 113) proved to be malignant; 89 (89.9%) lesions were primary lung cancer, seven (7.1%) were metastases, two (2.0%) were malignant lymphomas, and one (0.9%) was a mucosa-associated lymphoid tissue (MALT) lymphoma.

One lesion of inflammatory cell infiltration with ground-glass opacity was considered as an indeterminate lesion and was excluded because it could not be tracked in follow-up images.

Regarding the confirmation of the final diagnosis for malignancy, small cell carcinoma (n=1) was proven by both biopsy and surgical resections. The other 98 malignant lesions were diagnosed by biopsy.

Regarding the confirmation of the final diagnosis for benignancy, organizing pneumonia (n=1) was proven by both biopsy and surgical resection. The other 12 benign lesions were diagnosed with biopsies. Following the exclusion of the specific four lesions of tuberculosis, hamartoma, plasmacytoma, and amyloidosis, six lesions, including epithelioid granulomas (n=3), organized pneumonias (n=2), or inflammatory cell infiltration with fibrosis (n=1), revealed benign characteristics because they decreased more than 20% in diameter within the 1-year follow-up period; one epithelioid granuloma (n=1) was benign because it did not change in size dur-

ing the period that preceded the 2-year follow-up. There was one false positive biopsy in the ground-glass opacity lesions, which was pathologically demonstrated as an atypical cell infiltration malignancy. However, this lesion exhibited regression in follow-up CT examinations (≥2 years) without therapy. Therefore, the sensitivity for malignant lesions, specificity for benign lesions, and diagnostic accuracy, were 99/99 (100%), 12/13 (92.7%), and 111/112 (99.1%), respectively.

Air embolization, hemothorax, hemoptysis, pneumothorax, and pulmonary hemorrhagic complications respectively occurred in 0, 2, 12, 48, and 70 procedures. There were no patients with life-threatening and grade 3 pulmonary hemorrhage. Although pulmonary hemorrhage occurred in 50% (35/70) of the studied cases (>2 cm), these complications were self-limiting and non-life threatening.

Hemoptysis was graded as mild in 12 (10.6%) patients who had a brief period of hemoptysis. However, no patients required supportive care and therapeutic intervention.

Pneumothorax occurred in 48 procedures. It was graded as mild in 42 (87.5%), moderate in four (8.3%), and severe in two (4.2%) out of the 48 pneumothorax cases. One patient with severe pneumothorax was required to insert the chest tube for the air drainage. Five patients with clinical symptoms underwent manual evacuations.

Hemothorax occurred in two procedures during biopsy. The first lesion (Fig. 4) was a 55 mm metastatic tumor from the colon that abutted the pleura in the left lower lobe in a 70-year-old man with multiple hepatic metastases owing to colon cancer. The needle was progressed through the inferior position within the 10th intercostal space in the tail-head and medial-lateral directions. The distance from the spinous process to the pleura was 44 mm. Although the post-CBCT procedure did not demonstrate pleural blood effusion, the patient's blood pressure decreased, while the chest radiograph acquired 4 h after the procedure detected massive pleural effusion. Non-enhanced CT revealed massive blood effusion in the thorax. Contrast-enhanced dynamic CT images did not demonstrate the extravasation in the thorax and laceration and pseudoaneurysm in the left 10th intercostal artery. The chest tube was placed to drain the blood

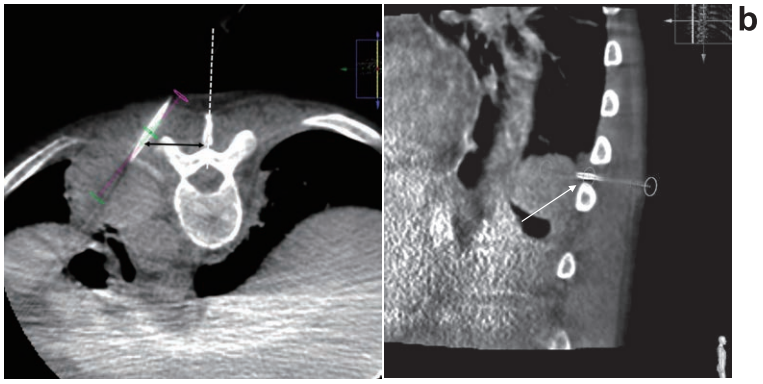

Fig. 4. A 55 mm lesion in the left lower lobe in a 70-year-old man

a : Axial CBCT image showing that the introducer has been advanced through the erector spinal muscles in the medial-lateral direction. The distance from the spinous process to the pleura is 44 mm (double arrow line).

b : Oblique sagittal image showing that the needle has been advanced through the inferior area (arrow) within the 10th intercostal space in the tail-head direction. Hemothorax was confirmed on chest CT images (not shown) 4 h after biopsy, and a chest tube was then inserted into the pleural space. The lesion was confirmed to be metastatic adenocarcinoma from rectal cancer.

pleural effusion. The patient's condition was stable. However, he died owing to liver failure one week after the procedure. The second lesion was a 31-mm MALT lymphoma that abutted the pleura in the left lower lobe in a 77-year-old man. The needle was progressed through the middle position within the 9th intercostal space in the tail-head and lateral-medial directions. The distance from the spinous process to the pleura was 52 mm. We noted the appearance of the pleural blood effusion during the procedure. However, the patient's vital signs were stable and CBCT did not exhibit pleural effusion increases during the procedure and 15 min after the procedure. Consequently, contrast-enhanced dynamic CT was not performed. The chest tube was not placed because a chest radiograph acquired 4 h after the procedure did not show signs of an increasing pleural effusion.

Assessing the risk factors for complications and technical parameters

Univariate analysis (Table 3) demonstrated that the small size ($p < 0.001$), lesion depth ($p = 0.038$), and longer distance of traversed aerated lung ($p = 0.017$), were independent risk factors for pulmonary hemorrhage. Multivariate analysis identified the small lesion size as an independent risk factor for pulmonary hemorrhage ($p = 0.001$).

Univariate analysis (Table 4) revealed that age ($p = 0.048$), presence of emphysema ($p = 0.042$), lesion size ($p = 0.011$), and direction of the needle progression ($p = 0.001$) were independent risk factors for pneumothorax. Multivariate analysis identified the age ($p = 0.013$), small size ($p = 0.008$), and direction of the needle progression ($p = 0.002$), as independent risk factors for pneumothorax.

Discussion

The CBCT system provides advanced needle planning with real-time needle guidance, in combination with multiplanar, 3D CBCT and fluoroscopy images[4, 7–12]. Therefore, CBCT-based 3D needle guidance allows variable angulated needle trajectories and permits advancement for small (≤ 2 cm) pulmonary lesions[11].

To our knowledge, our study is the first report with a) quantitative and qualitative evaluations of the pleural puncture sites within the intercostal space, and b) the capacity to direct the needles to avoid hemothorax owing to the laceration of PIA with CBCT-guided TLB. The incidence of hemothorax in this study was 1.8% (2 / 113), and corresponded with previous studies that reported incidence rates in the range of 1.62–1.8%[18, 28].

We did not perform any procedures in the superior intercostal spaces (inferior edge of the rib). Regarding our goal to locate a pleural puncture location at > 6 cm lateral to the spinous processes at all the spinal levels, only 35 of 113 (30.9%) procedures allowed its requirement: 5 of 24 (20.8%) were in the 2nd to the 3rd intercostal spaces, 11 of 45 (24.4%) were in 4th to the 7th intercostal spaces, and 19 of 44 (43.2%) were in the 8th to the 11th intercostal spaces. Despite these technical parameters, hemothorax occurred in only two procedures, and the remaining 111 of 113 (98.2%) procedures did not cause hemothorax. Although the courses of PIAs in the posterior medial lower back are unpredictable[6], PIAs may be anatomically located in the inferior half of the intercostal space in the posterior medial chest[14], especially at the lower

thoracic level[16]. Moreover, PIAs tends to be more tortuous in older patients[15]. This hypothesis was confirmed because hemothorax occurred in the posterior approach at the 10th and 9th intercostal spaces with corresponding distances of 44 mm and 52 mm from the spinous process with respect to the corresponding pleura.

Regarding diagnostic yield, in this study, diagnostic accuracy, sensitivity, and specificity were 99.1%, 100%, and 92.3%, for all pulmonary lesions, respectively. These results were similar to or higher than those reported in previous CBCT-guided TLB studies that yielded 90–98% diagnostic accuracy, 94–97% sensitivity, and 75–100% specificity[2, 3, 5, 7–12]. In our procedures, the incidence of pneumothorax, pulmonary hemorrhage, and hemorrhage $>$ 2 cm was 42.5% (48 / 113), 61.9% (70 / 113), and 31.0% (35 / 113), respectively. To compare with the previous reports that used CT- or CT-fluoroscopic guidance, the incidence of pneumothorax in our study was slightly higher and in the range of 8.6–42.3%[18, 29–31]. We suspect that a small amount of pneumothorax can be detectable in high-resolution, post-CBCT scans. The frequency of the air drainage for pneumothorax using manual evacuation and chest tube placement was 5.3% (6 / 113). This was smaller than the previous reports (11.9–13.1%)[31, 32] that used 19 or 20-gauge coaxial cutting needles.

The incidence of pulmonary hemorrhage after TLB in previous studies was high and in the range of 9.9–65.6%[29]. It was believed that this high-diagnostic performance and high-complication rates resulted from the multiple sampling using the coaxial system and CBCT-guidance without on-site pathologists, irrespective of the lesion type[17].

Based on multivariate analyses, we inferred that a smaller lesion size constitutes an independent risk factor for pulmonary hemorrhage. The result was similar to the finding in a previous report[30] that stated that small lesion sizes constituted one of the most frequently reported risk factors for pulmonary hemorrhage. Yeow *et al*[17] speculated that a higher hemorrhage rate occurred in patients with lesions which were smaller than 20 mm. The chosen value corresponded to the throw length of most cutting needles. Additionally, Chassagnon *et al*[27] reported that a coaxial needle tip outside the target lesion correlated with increased hemoptysis. Correspondingly, we agree that pulmonary hemorrhage after TLB may be a secondary complication following the extension of the cutting needle into the normal, surrounding lung parenchyma in small lesions[17, 27, 29]. In addition, we speculated that the multiple sampling achieved by tilting the system slightly at every needle pass to obtain 3–5 biopsy samples, could induce more frequent hemorrhage.

Based on univariate analyses, we found that the lesion depth and the distance of traversed aerated lung were associated with pulmonary hemorrhage. Results showed that targeted lesions were separated from the pleuras, and the distances of traversed aerated lung achieved with the introducer needles were large. The distance of the traversed aerated lung was 26.7 ± 14.5 mm in this study, which was longer than the distance of 17 ± 17 mm reported previously[8, 22, 27]. The increased hemorrhage could correspond to an increased distance of traversed lung parenchyma and to an increased risk of pulmonary vessel damages[19].

The incidence of hemoptysis in our study was 10.6%. This rate was similar to the rates reported by Wu *et al*[24] (11%), and Choi *et al*[21] (14.5%). Blood mixed in phlegm was classified as mild and self-limiting hemoptysis in our study.

There are several limitations associated with this study. First, this study was a retrospective study. Accordingly, prospective trials are required. Second, CBCT images are acquired with the patients in the prone position at the end of expiration. These differ from the recent diagnostic CT images acquired from patients in supine positions at the end of inspiration. Thus, the anatomical features, including intercostal arteries in the intercostal spaces, could vary based on the patient's position. Third, the population number was small, and included a limited number (n=4) of ground-glass opacity lesions. Other patient populations should also be investigated.

Conclusions

In this study, CBCT-guided TLB with a posterior intercostal approach yielded high diagnostic accuracy with low complication rates. Radiologists should understand the potential risk of hemothorax secondary to laceration of the PIA that may be located in the inferior halves of the intercostal spaces in TLB cases for lesions in the medial chest.

Conflict of interest disclosure

The authors declare no conflicts of interest regarding this study.

References

1) Sharma A, Shepard JO. Lung Cancer Biopsies. *Radiol Clin North Am*. 2018;**56**:377-390.
2) Fior D, Vacirca F, Leni D, *et al*. Virtual guidance of percutaneous transthoracic needle biopsy with C-arm cone-beam CT: diagnostic accuracy, risk factors and effective radiation dose. *Cardiovasc Intervent Radiol.* 2019;**42**:712-719.
3) Lee SM, Park CM, Lee KH, *et al*. C-arm cone-beam CT-guided percutaneous transthoracic needle biopsy of lung nodules: clinical experience in 1108 patients. *Radiology.* 2014;**271**:291-300.
4) Rotolo N, Floridi C, Imperatori A, *et al*. Comparison of cone-beam CT-guided and CT fluoroscopy-guided transthoracic needle biopsy of lung nodules. *Eur Radiol*. 2016;**26**:381-389.
5) Jin KN, Park CM, Goo JM, *et al*. Initial experience of percutaneous transthoracic needle biopsy of lung nodules using C-arm cone-beam CT systems. *Eur Radiol*. 2010;**20**:2108-2115.
6) Tsai IC, Tsai WL, Chen MC, *et al*. CT-guided core biopsy of lung lesions: a primer. *AJR Am J Roentgenol*. 2009;**193**:1228-1235.
7) Choi MJ, Kim Y, Hong YS, *et al*. Transthoracic needle biopsy using a C-arm cone-beam CT system: diagnostic accuracy and safety. *Br J Radiol*. 2012;**85**:e182-e187.
8) Lee WJ, Chong S, Seo JS, *et al*. Transthoracic fine-needle aspiration biopsy of the lungs using a C-arm cone-beam CT system: diagnostic accuracy and post-procedural complications. *Br J Radiol*. 2012;**85**:e217-e222.
9) Braak SJ, Herder GJ, van Heesewijk JP, *et al*. Pulmonary masses: initial results of cone-beam CT guidance with needle planning software for percutaneous lung biopsy. *Cardiovasc Intervent Radiol.* 2012;**35**:1414-1421.
10) Choi JW, Park CM, Goo JM, *et al*. C-arm cone-beam CT-guided percutaneous transthoracic needle biopsy of small (≤20 mm) lung nodules: diagnostic accuracy and complications in 161 patients. *AJR Am J Roentgenol*. 2012;**199**:W322-W330.
11) Choo JY, Park CM, Lee NK, *et al*. Percutaneous transthoracic needle biopsy of small (≤1 cm) lung nodules under C-arm cone-beam CT virtual navigation guidance. *Eur Radiol.* 2013;**23**:712-719.
12) Jiao de C, Li TF, Han XW, *et al*. Clinical applications of the C-arm cone-beam CT-based 3D needle guidance system in performing percutaneous transthoracic needle biopsy of pulmonary lesions. *Diagn Interv Radiol*. 2014;**20**:470-474.

13) Yoneyama H, Arahata M, Temaru R, *et al*. Evaluation of the risk of intercostal artery laceration during thoracentesis in elderly patients by using 3D-CT angiography. *Intern Med*. 2010;**49**:289–292.
14) Choi S, Trieu J, Ridley L. Radiological review of intercostal artery: anatomical considerations when performing procedures via intercostal space. *J Med Imaging Radiat Oncol*. 2010;**54**:302–306.
15) Dewhurst C, O'Neill S, O'Regan K, *et al*. Demonstration of the course of the posterior intercostal artery on CT angiography: relevance to interventional radiology procedures in the chest. *Diagn Interv Radiol*. 2012;**18**:221–224.
16) Helm EJ, Rahman NM, Talakoub O, *et al*. Course and variation of the intercostal artery by CT scan. *Chest*. 2013;**143**:634–639.
17) Yeow KM, See LC, Lui KW, *et al*. Risk factors for pneumothorax and bleeding after CT-guided percutaneous coaxial cutting needle biopsy of lung lesions. *J Vasc Interv Radiol*. 2001;**12**:1305–1312.
18) Wang Y, Jiang F, Tan X, *et al*. CT-guided percutaneous transthoracic needle biopsy for paramediastinal and non-paramediastinal lung lesions: diagnostic yield and complications in 1484 patients. *Medicine (Baltimore)*. 2016;**95**:e4460. (accessed 2019 Jul 15) Available from: https://www.ncbi.nlm.nih.gov/pmc/articles/PMC4979835/pdf/medi-95-e4460.pdf
19) Nour-Eldin NE, Alsubhi M, Emam A, *et al*. Pneumothorax complicating coaxial and non-coaxial CT-guided lung biopsy: comparative analysis of determining risk factors and management of pneumothorax in a retrospective review of 650 patients. *Cardiovasc Intervent Radiol*. 2016;**39**:261–270.
20) Wallace MJ, Krishnamurthy S, Broemeling LD, *et al*. CT-guided percutaneous fine-needle aspiration biopsy of small (< or = 1-cm) pulmonary lesions. *Radiology*. 2002;**225**:823–828.
21) Choi SH, Chae EJ, Kim JE, *et al*. Percutaneous CT-guided aspiration and core biopsy of pulmonary nodules smaller than 1 cm: analysis of outcomes of 305 procedures from a tertiary referral center. *AJR*. 2013;**201**:964–970.
22) Yildirim E, Kirbas I, Harman A, *et al*. CT-guided cutting needle lung biopsy using modified coaxial technique: factors effecting risk of complications. *Eur J Radiol*. 2009;**70**:57–60.
23) Lal H, Neyaz Z, Nath A, *et al*. CT-guided percutaneous biopsy of intrathoracic lesions. *Korean J Radiol*. 2012;**13**:210–226.
24) Wu RH, Tzeng WS, Lee WJ, *et al*. CT-guided transthoracic cutting needle biopsy of intrathoracic lesions: comparison between coaxial and single needle technique. *Eur J Radiol*. 2012;**81**:e712–e716.
25) Hiraki T, Fujiwara H, Sakurai J, *et al*. Nonfatal systemic air embolism complicating percutaneous CT-guided transthoracic needle biopsy: four cases from a single institution. *Chest*. 2007;**132**:684–690.
26) Tai R, Dunne RM, Trotman-Dickenson B, *et al*. Frequency and severity of pulmonary hemorrhage in patients undergoing percutaneous CT-guided transthoracic lung biopsy: single-institution experience of 1175 cases. *Radiology*. 2016;**279**:287–296.
27) Chassagnon G, Gregory J, AI Ahmar M, *et al*. Risk factors for hemoptysis complicating 17-18 gauge CT-guided transthoracic needle core biopsy: multivariate analysis of 249 procedures. *Diagn Interv Radiol*. 2017;**23**:347–353.
28) Mills M, Choi J, El-Haddad G, *et al*. Retrospective analysis of technical success rate and procedure-related complications of 867 percutaneous CT-guided needle biopsies of lung lesions. *Clin Radiol*. 2017;**72**:1038–1046.
29) Freund MC, Petersen J, Goder KC, *et al*. Systemic air embolism during percutaneous core needle biopsy of the lung: frequency and risk factors. *BMC Pull Med*. 2012;**12**:2. (accessed 2019 Jul 15) Available from: https://www.ncbi.nlm.nih.gov/pmc/articles/PMC3608336/pdf/1471-2466-12-2.pdf
30) Heerink WJ, de Bock GH, de Jonge GJ, *et al*. Complication rates of CT-guided transthoracic lung biopsy: meta-analysis. *Eur Radiol*. 2017;**27**:138–148.
31) Hiraki T, Mumura H, Gohara H, *et al*. Incidence of and risk factors for pneumothorax and chest tube placement after CT fluoroscopy-guided percutaneous lung biopsy: retrospective analysis of the procedures conducted over a 9-year period. *AJR Am J Roentgenol*. 2010;**194**:809–814.
32) Kuban JD, Tam AL, Huang SY, *et al*. The effect of needle gauge on the risk of pneumothorax and chest tube placement after percutaneous computed tomographic (CT)-guided lung biopsy. *Cardiovasc Intervent Radiol*. 2015;**38**:1595–1602.

[Received January 20, 2020 : Accepted March 5, 2020]